

ENCLOSURE

FINAL REPORT

DIABLO CANYON UNIT 2
TURBINE BUILDING OPERATING DECK

PACIFIC GAS AND ELECTRIC COMPANY

JUNE 1985

REGULATORY DOCKET FILE COPY

0345S/0033K

8506110082	850606
PDR	ADOCK 05000323
E	PDR

1940s and 1950s

TABLE OF CONTENTS

1. Background and Introduction
2. Description of Floor System at Elevation 140 Feet
3. Turbine Building Classification and Design Criteria
4. Detailed Analysis and Evaluation
5. Summary and Conclusions
6. References

TABLES

1. Hosgri Evaluation
2. FINEL Analysis Forces, Strains, and Stresses, Hosgri Load Acting in the West Direction, Concrete Considered Uncracked
3. FINEL Analysis Forces, Strains, and Stresses, Hosgri Load Acting in the West Direction, Concrete Considered Cracked
4. FINEL Analysis Forces, Hosgri Load Acting in the East Direction

FIGURES

1. Turbine Building Unit 2, Concrete Floor System at El. 140'-0"
2. Turbine Building Unit 2, Section 'A'
3. Unit 2 Turbine Building, Elev. 140 Ft. Floor Diaphragm, FINEL Analysis Model

ATTACHMENT

- A. Description of Computer Program CE 801 (FINEL)



1. Background and Introduction

As part of the Diablo Canyon Unit 2 design completion and design verification program, calculations and analyses were performed by the Diablo Canyon Project (DCP) to verify that the Unit 2 turbine building would withstand the effects of the postulated Hosgri earthquake. During routine DCP review and approval of calculations evaluating the strength of the turbine operating deck concrete floor slab diaphragm (elevation 140 feet), an area of potential nonlinear behavior was identified. This potential nonlinear behavior involved shear force transfer through a relatively small region of the turbine operating deck between the north end of the turbine pedestal and the opening for the freight elevator as shown on Figure 1. Nonlinear behavior in a seismic event is allowed by the turbine building criteria for Diablo Canyon as defined in the Hosgri Report, based on its status as a Seismic Design Class II structure upgraded to assure continued functioning of certain Seismic Design Class I equipment housed therein. However, the NRC Staff, in previous safety evaluation report supplements, has requested that such nonlinear behavior be justified for each specific case, and that such justification be presented for Staff review. The purpose of this report is to discuss the behavior of this area of the turbine operating deck, its further evaluation, and PGandE's conclusion that the structure is qualified to withstand the postulated Hosgri seismic conditions.

PGandE's initial assessment of the structural behavior of this region of the turbine operating deck was discussed during a meeting with the NRC Staff at the time of their audit in San Francisco on January 15, 1985. At this time, the mode of behavior of special interest was one of shear friction. During the meeting it was pointed out by the DCP that their initial assessment included certain conservatisms such that the suspected nonlinear behavior might not actually exist. Furthermore, even if local nonlinear behavior was found to exist, the impact on overall structural behavior and response of the building would be expected to be quite limited. Also, during the meeting, it was reported by the DCP that a similar condition did not exist in Unit 1, based on the different physical arrangement of Unit 1 and detailed calculations evaluating the corresponding region of the turbine operating deck in Unit 1.

It was agreed during the meeting that this investigation need not be completed prior to low power operation of Unit 2 for the following reasons: (1) The effect of the increase in deformation due to potential shear nonlinearity would be confined to a very local area. (2) No Category 1 equipment or systems are attached to the turbine operating deck slab in the local area. (3) The potential increase in deformation would be too small to affect the response of Category 1 equipment attached to the turbine operating deck slab at other locations.

During a second meeting with the NRC Staff at Brookhaven National Laboratory (BNL) on March 16, 1985, preliminary results of further studies were discussed by the DCP. These studies included investigations



of the shear friction mode of behavior at the critical section, the availability of diagonal shear capacity greater than the code value, the effects of concrete cracking and redistribution of forces to steel reinforcing and floor framing members, and availability of greater strength as a result of concrete aging. Results reported were that the governing mode of shear failure is the diagonal shear mode rather than that of shear friction, and that diagonal shear capacity, using appropriate test data, exceeds the design shear force without considering the beneficial effect of concrete aging. It was also reported that the preliminary results show that the effects of concrete cracking would be limited additional displacement and redistribution of forces which could be readily accommodated by the structural system.

The following sections of the report provide a detailed description of the turbine operating deck floor system, design criteria, final results of evaluations performed, and conclusions, as presented during the NRC audit of May 30 and 31, 1985.

2. Description of Floor System at Elevation 140 Feet

The turbine operating deck floor (elevation 140 feet) for the Unit 2 turbine building is a 12-inch-thick reinforced concrete slab supported vertically by steel framing members which are supported on steel columns and concrete walls. The floor, acting as a horizontal diaphragm to resist seismic loadings, is supported in the horizontal direction by concrete walls at column lines 19, 31, A, and G. In addition to the large turbine pedestal opening at the interior of the floor, numerous openings in the floor exist at equipment hatches, stairwells, piping and duct penetrations, and at the freight elevator. A plan of the floor system showing concrete outlines, openings, floor diaphragm chord beams, and concrete walls below is shown on Figure 1.

The floor section of interest with the floor acting as a horizontal diaphragm is at column line C between column lines 19 and 21. At this location the floor continuity is interrupted by the relatively large freight elevator opening. A section through the floor at this location is shown in Figure 2.

The corresponding turbine operating deck floor at the south end of the Unit 1 turbine building is similar, except that the floor is two bays longer, the freight elevator opening is not present, and a more effective embedded framing system for resisting shear forces is present.

3. Turbine Building Classification and Design Criteria

The turbine building is a Seismic Design Class II structure. However, certain Design Class I equipment such as the component cooling water (CCW) heat exchangers, 4160V vital switchgear, emergency diesel generators, and associated systems are located within the structure. The CCW heat exchangers, located between lines 19 and 22 and E and F, and



diesel generators, located between lines 32 and 35 and A and D, are supported on the foundation slab at elevation 85 feet and, therefore, are not directly affected by the building response. The 4160V vital switchgear, located between lines 32 and 35 and E and G are supported on the floor at elevation 119 feet. Associated Class I systems are generally supported on floors at elevation 119 feet and below, with the exception of the control room pressurization system and the onsite technical support center pressurization system which are supported along the east, west, and south edges of the turbine operating deck concrete floor at elevation 140 feet.

To provide assurance that the function of Design Class I equipment will not be adversely affected in the event of the postulated Hosgri earthquake, the turbine building is analyzed to ensure the building does not collapse and equipment would not be affected by any failure of the structure. These requirements are specified in the FSAR, Sections 3.7 and 3.8 and the Hosgri Report, Section 4.4.

The turbine building analysis uses the same free field ground motion as is used for Design Class I structures. Analysis procedures are the same as those for Class I structures except that response may be determined by both linear elastic and nonlinear inelastic methods. Inelastic response is limited to ductilities in concrete below 1.3 (Ref. Hosgri Report Section 4.1.3). These criteria are consistent with the assumption that limited local structural damage is permissible provided that overall safety of the Class I equipment is not impaired.

Allowable stresses for reinforced concrete elements except shear walls are as given in ACI 318-71 and the 1973 supplement thereto (ACI 318-73). Allowable stresses in concrete shear walls are as stated in "Recommended Lateral Force Requirements, 1974 Seismology Committee Structural Engineers Association of California (SEAOC), "Section 3(C), "Shear and Diagonal Tension Strength Design." Lateral force resisting elements are allowed inelastic deformations according to those indicated in Table 4-2 of the Hosgri Report. For these elements, the allowable stress limitations of ACI 318 and SEAOC need not apply. (Ref. Hosgri Report Section 4.1.4).

4. Detailed Analysis and Evaluation

Forces at the critical section were obtained from the dynamic analysis of the three-dimensional model of the turbine building. The forces were compared to capacities determined by the methods of ACI 318-73, Section 11.16. The forces used do not include the effects of load redistribution due to the limited tension capacity of concrete. As discussed later in this section, these effects reduce tension and shear forces at the critical section.

Neither the FSAR nor the Hosgri Report contain criteria referring specifically to floor diaphragms. The Hosgri Report prescribed



ACI 318-73 as the code applicable to concrete elements except shear walls. As this code does not contain specific provisions for floor diaphragms, special provisions for walls contained in Section 11.16 of the code were used to calculate the shear capacity. The calculation uses average 60-day test strength of the concrete, and a capacity reduction factor of 0.85. For this conservative set of conditions, when earthquake loads are acting in the west direction, the shear demand exceeds the shear capacity as shown on Table 1. As shown in the table, axial force and moment capacities are greater than the applied forces.

In determining the forces at the critical section, the three-dimensional linear elastic dynamic analysis considers the floor at elevation 140 feet as a homogeneous elastic medium capable of resisting compression and tension. In reality, the floor system is nonhomogeneous, consisting of concrete having a relatively low tension capacity reinforcing bars spread throughout the floor, and structural steel beams and girders at discrete locations. When forces acting on a section induce tension in the concrete beyond the tensile limit of the concrete, the concrete will crack and redistribute the forces to the steel elements. As the conservative evaluation using the dynamic model forces indicated excessive shear demand, additional analysis accounting for the force redistribution due to concrete cracking was performed.

The additional analysis is a static analysis using the FINEL computer program to determine forces at the critical section resulting from a Hosgri earthquake in the east-west direction. The FINEL program is described in Attachment A. The analysis used a model of the turbine operating deck floor at elevation 140 feet consisting of a fine mesh of rectangular plane stress elements. Separate elements were used to model the concrete, the reinforcing bars, and the structural steel beams. Model boundaries were selected as column lines A, G, 19, and 35. Stiffnesses of the concrete walls at column lines A, G, 19, and 31 were included. Nonlinear material properties were specified to account for limited tensile capacity of the concrete and yield capacity of the reinforcing bars and steel beams.

Loads applied to the model were the inertia loads equal to the product of nodal masses and nodal accelerations in the east-west direction. These data were obtained from the three-dimensional linear elastic dynamic analysis of the turbine building for the case of the bridge cranes located near the north end of the Unit 2 turbine building. Two load cases were analyzed: (1) loads acting from east to west, inducing tension on the critical section, and (2) loads acting west to east, inducing compression on the section.

Results of the analysis were obtained for the uncracked condition, corresponding to the behavior considered in the dynamic analysis, and for the cracked condition corresponding more closely to the actual behavior. For the uncracked condition, shear at the critical section is close to the value obtained from the dynamic analysis. For the cracked condition,



the shear and normal forces at the critical section are significantly lower. Results of the analysis for both load cases, for both the uncracked and cracked condition, are shown in Tables 2, 3, and 4. It can be seen that applied forces at the critical section are less than the yield capacity. Table 3 shows the concrete crack angle in pier 1 based on principal stress, measured counter-clockwise from line C, to be between 20 and 40 degrees. This analysis verifies that the shear friction mode of failure is precluded because no horizontal crack along column line C is formed.

Shear forces obtained by the analysis, for the cracked condition, were compared to the shear capacities based on the methods of ACI 318-73, Section 11.16 considering no concrete aging. The comparison, shown in Table 1, shows the shear capacity exceeds the shear force at the section.

Normal force and moment determined by the analysis are also compared to the section's capacity. The comparison, shown in Table 1, shows the moment capacity of the section in the presence of the calculated normal force is more than twice the calculated moment.

It is recognized that the comparison shown in Table 1 includes additional conservatism relating to the effect of aging on concrete strength and capacity reduction factors. Also, it is recognized that ACI 318-73, Section 11.16 shear capacities are very conservative for panels having a low aspect ratio, as discussed in Reference 1.

5. Summary and Conclusions

The portion of the turbine building deck (elevation 140 feet) described in Section 2 has been analyzed with the results summarized in Table 1. The analysis indicates there is adequate capacity to resist the expected loads from the postulated Hosgri earthquake. The analysis indicates the shear friction mode of behavior is not controlling.

The evaluation of the deck does not take credit for greater strength that is available when considering the effects of concrete aging, more realistic capacity reduction factors, and panel test behavior with low aspect ratio. Additional conservatism is the energy absorbing capability of the structure during inelastic deformation resulting from yielding of the reinforcing steel. The structure has the ability to deform inelastically because of the relatively low steel ratios and adequate structural steel and reinforcing steel details.

The Hosgri Report, Table 4-2, allows the response spectra to be determined by linear elastic analysis with a ductility factor up to 1.3. The detailed analyses show that the capacities based on 60-day concrete strength and the code capacity reduction factor exceed the demands determined by linear elastic analyses. Since the capacity of the section is controlled by shear, the strain in the reinforcing steel is less than yield. The FINEL analysis also predicts the strain in the reinforcing



steel is less than yield. All of these analyses indicate the ductility is below 1.0, which is well below 1.3, therefore, previously determined response spectra remain adequate for equipment and systems qualification.

From these analyses considering both strength and deformation, it is concluded that the turbine building deck section discussed herein is properly qualified.

6. References

1. "Shear Strength of Low-Rise Walls with Boundary Elements," by Felix Barda, John M. Hanson and W. Gene Corley, Reinforced Concrete Structures in Seismic Zones, Publication SP-53. American Concrete Institute, Detroit.

2. Drawings

Equipment Location Drawings

500964 Plan At Elevation 85'-0"
500965 Plan At Elevation 104'-0"
500966 Plan At Elevation 119'-0"
500967 Plan At Elevation 140'-0"

Turbine Building Design Drawings

438342 Structural Steel Plan Elevation 140'-0" South
443062 Concrete Outline Plan Elevation 140'-0", Areas "B", "C" & "D"
443086 Reinforcing Plan Elevation 140'-0", Areas "B", "C" & "D"
443116 Structural Steel Plan of Elevation 140'-0" North
444810 Wall Openings, Elevation 85'-0" to 140'-0" (Col. Line 19)

Turbine Building Erection and Fabrication Drawings

Structural Steel, Unit 2 DC 663381, Sheet Nos. 61, 62, 157, 158, 213, 363, 374
Structural Steel, Unit 1 (Line 19) DC 663237, Sheet Nos. 252, 636, 640, 641, 695
Reinforcing Steel, Unit 2 DC 663367, Sheet Nos. 602 to 606



TABLE 1

Unit 2 Turbine Building
Floor Diaphragm at Elevation 140 Feet
Hosgri Evaluation

Model	Earthquake Direction	Force	Demand(a)	Capacity(c)(d)(e)
3-D Dynamic Analysis Model	E-W	Axial, T ₁	1,650 k(tension)	(b)
		Axial, T ₂	1,290 k(tension)	(b)
		Shear, V	2,780 k	2,370 k
		Moment, M(g)	10,400 k-ft	72,900 k-ft
	W-E	Axial, T ₁	1,650 k(compression)	(b)
		Axial, T ₂	1,290 k(compression)	(b)
2-D FINEL Model (f)	E-W	Axial, T ₁	200 k(compression)	(b)
		Axial, T ₂	2,160 k(tension)	(b)
		Moment, M(g)	37,000 k-ft	92,000 k-ft
		Shear, V	1,850 k	2,700 k

- (a) Demand forces represent SRSS of two horizontal earthquake directions.
- (b) Axial demand force effect is included in calculating shear and moment capacity.
- (c) Shear capacity is calculated by method of ACI 318-73, Section 11.16.
- (d) Shear capacity reduction factor used is 0.85.
- (e) Concrete strength used is average 60-day test strength.
- (f) FINEL model forces consider concrete cracking. Forces for case of earthquake in east direction are not shown as this case does not govern.
- (g) Moment is calculated at centerline of the section.

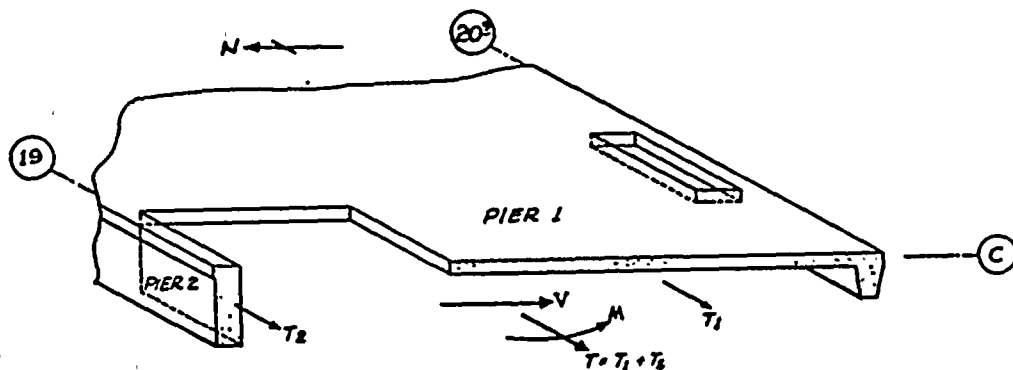




TABLE 2

Unit 2 Turbine Building
Floor Diaphragm at Elevation 140 Feet
FINEL Analysis Forces, Strains, and Stresses
Hosgr1 Load Acting in the West Direction
Concrete Considered Uncracked

MATERIAL	Resultant Forces ^(a)			Element No. ^(b)	Shear		Principal Strains and Stresses				Angle (Degrees)	
	Normal Force (Kips)	Moment (Kip-in)	Shear Force (Kips)		Strain x 10 ⁻³	Stress (psi)	Maximum		Minimum		Principal Strain	Principal Stress
							Strain 10 ⁻³	Stress (psi)	Strain x 10 ⁻⁴	Stress (psi)		
STEEL	279	-7980	-2	2233	-.029	-4	.104	3063	-.18	0	-83	-90
				2237	-.256	-38	.093	-1	-1.63	-1045	-45	-2
				2238	-.305	-45	.175	874	-1.31	-2	-46	-87
				2239	-.258	-38	.164	610	-.96	-2	-42	-86
				2240	-.255	-38	.175	1142	-.81	-1	-43	-88
				2241	-.300	-44	.213	1888	-.87	-1	-45	-89
				2242	-.288	-43	.238	3386	-.54	-1	-49	-89
CONCRETE	1970	-199000	-2630	3301	-.029	-56	.104	480	-.18	11	-83	-83
				3305	-.256	-490	.093	289	-1.63	-692	-45	-45
				3306	-.305	-585	.175	713	-1.31	-460	-46	-46
				3307	-.258	-495	.164	693	-.97	-303	-42	-42
				3308	-.255	-489	.175	763	-.81	-218	-43	-43
				3309	-.300	-576	.213	939	-.87	-212	-45	-45
				3310	-.288	-553	.238	1089	-.54	-29	-49	-49
TOTAL	2249	-206980	-2632									

(a) For force location and sign convention, see Detail 1, Figure 3.

(b) For element number identification, see Figure 3.



TABLE 3

Unit 2 Turbine Building
Floor Diaphragm at Elevation 140 Feet
FINEL Analysis Forces, Strains, and Stresses
Hogri Load Acting in the West Direction
Concrete Considered Cracked

MATERIAL	Resultant Forces ^(a)			Element No. ^(b)	Shear		Principal Strains and Stresses				Angle (Degrees)	
	Normal Force (Kips)	Moment (Kip-in)	Shear Force (Kips)		Strain x 10 ⁻³	Stress (psi)	Maximum		Minimum		Principal Strain	Principal Stress
							Strain 10 ⁻³	Stress (psi)	Strain x 10 ⁻⁴	Stress (psi)		
STEEL	3270	-457000	-10	2233	-.948	-124	1.82	46111	-.13	-.4	-74	-90
				2237	-1.430	-212	1.03	10531	-4.11	-4.3	-47	-89
				2238	-1.200	-177	1.07	18825	-2.00	-1.7	-54	-90
				2239	-.936	-137	1.01	22214	-.77	-.9	-60	-90
				2240	-.812	-118	1.00	24165	-.46	-.6	-65	-90
				2241	-.724	-106	.87	20569	-.23	-.6	-63	-90
				2242	-.340	-49	.70	19698	-.07	-.1	-76	-90
CONCRETE	-1310	38500	-1740	3301	-.948	-91	1.82	64.9	-.14	-119	-74	-40
				3305	-1.430	-943	1.03	.1	-4.11	-1888	-47	-47
				3306	-1.200	-433	1.07	.9	-2.00	-921	-54	-55
				3307	-.936	-143	1.01	2.0	-.77	-357	-60	-64
				3308	-.812	-70	1.00	2.1	-.46	-212	-65	-70
				3309	-.724	-27	.87	7.5	-.23	-111	-63	-77
				3310	-.340	46	.70	52.8	-.07	-78	-76	68
TOTAL	1960	-418500	-1750									

(a) For force location and sign convention, see Detail 1, Figure 3.

(b) For element number identification, see Figure 3.



TABLE 4

Unit 2 Turbine Building
 Floor Diaphragm at Elevation 140 Feet
 FINEL Analysis Forces
 Hosgri Load Acting in the East Direction

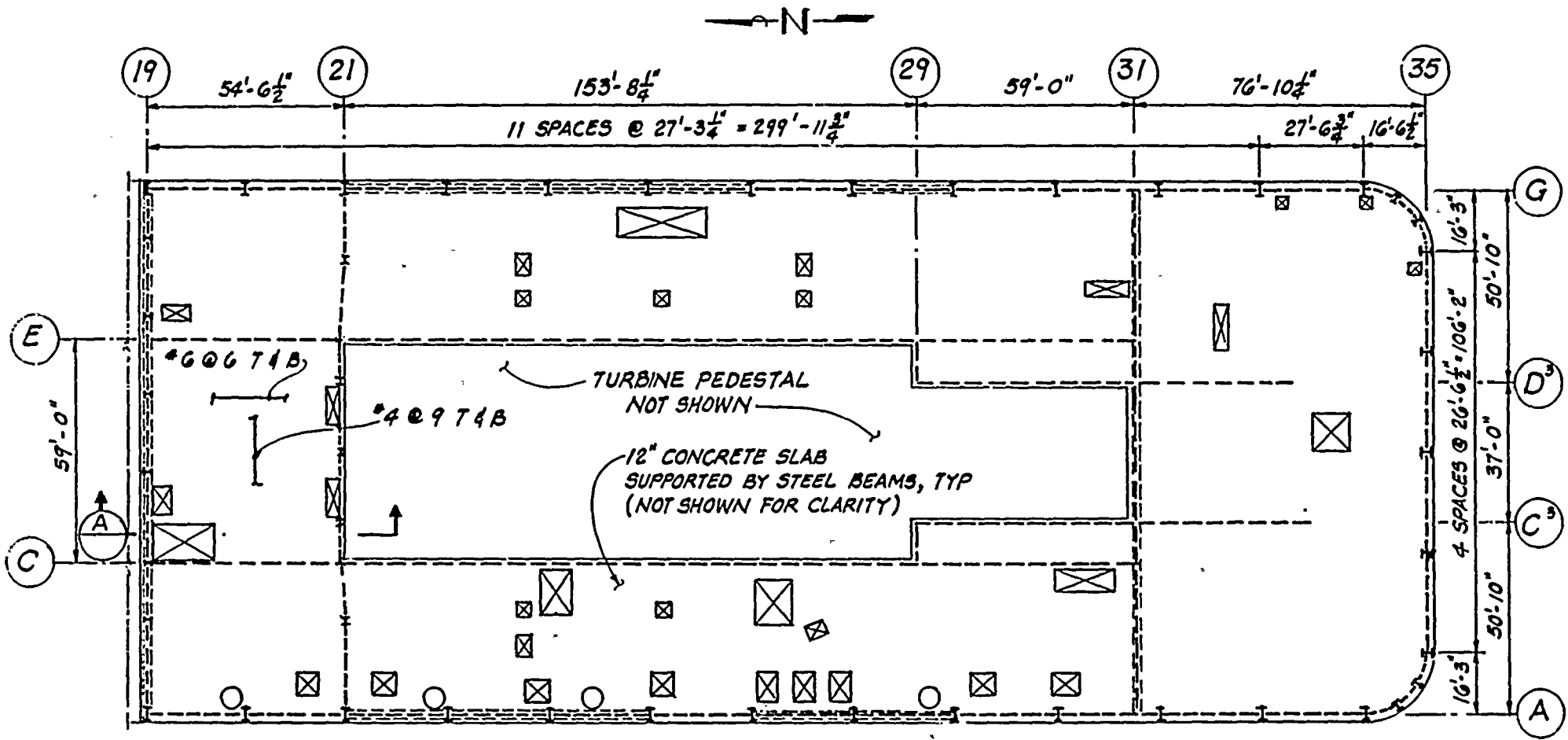
Resultant Forces (a)

Concrete Condition	Material	Normal Force (Kips)	Moment (Kip-in)	Shear Force (Kips)
Uncracked	Steel	-320	20,800	2
	Concrete	-1,930	188,000	2,626
	Total	-2,250	208,800(b)	2,628
Cracked	Steel	-195	49,100	2
	Concrete	-1,886	268,000	2,095
	Total	-2,081	317,100(b)	2,097

(a) For force location and sign convention, see Detail 1, Figure 3.

(b) Moment is calculated at centerline of the section between column lines 19 and 20.9.





LEGEND:

- CONTINUOUS CHORD BEAMS
- ===== SHEAR WALL

FIGURE 1
TURBINE BUILDING UNIT 2
CONCRETE FLOOR SYSTEM @
EL. 140'-0"



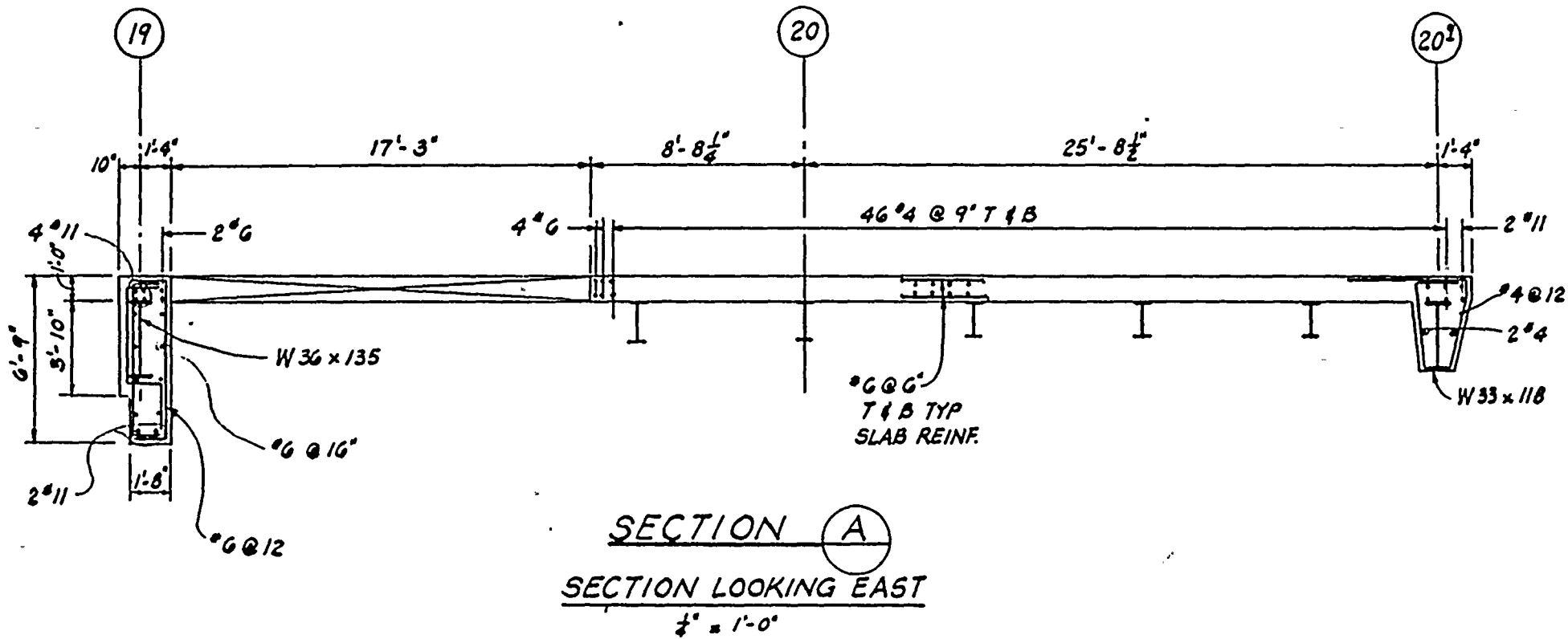
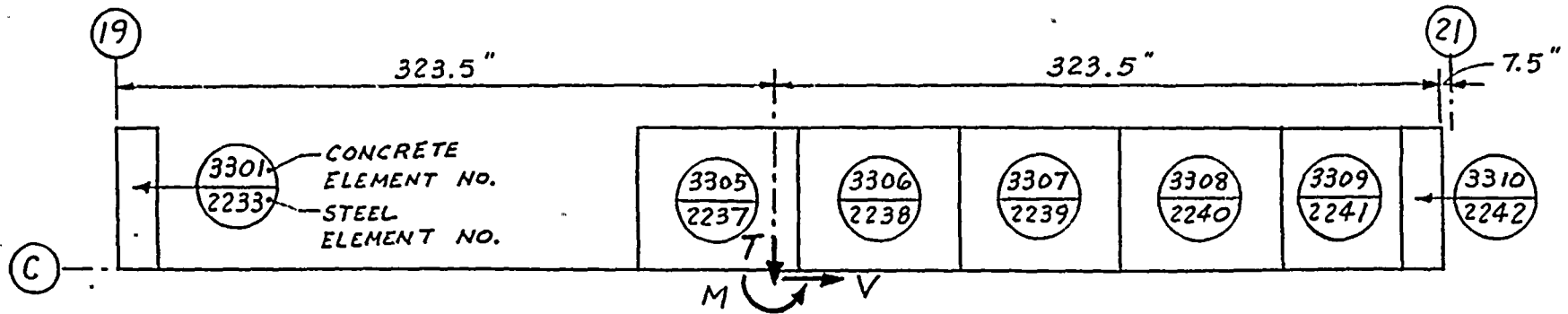


FIGURE 2
 TURBINE BUILDING UNIT 2
 SECTION 'A'





DETAIL 1

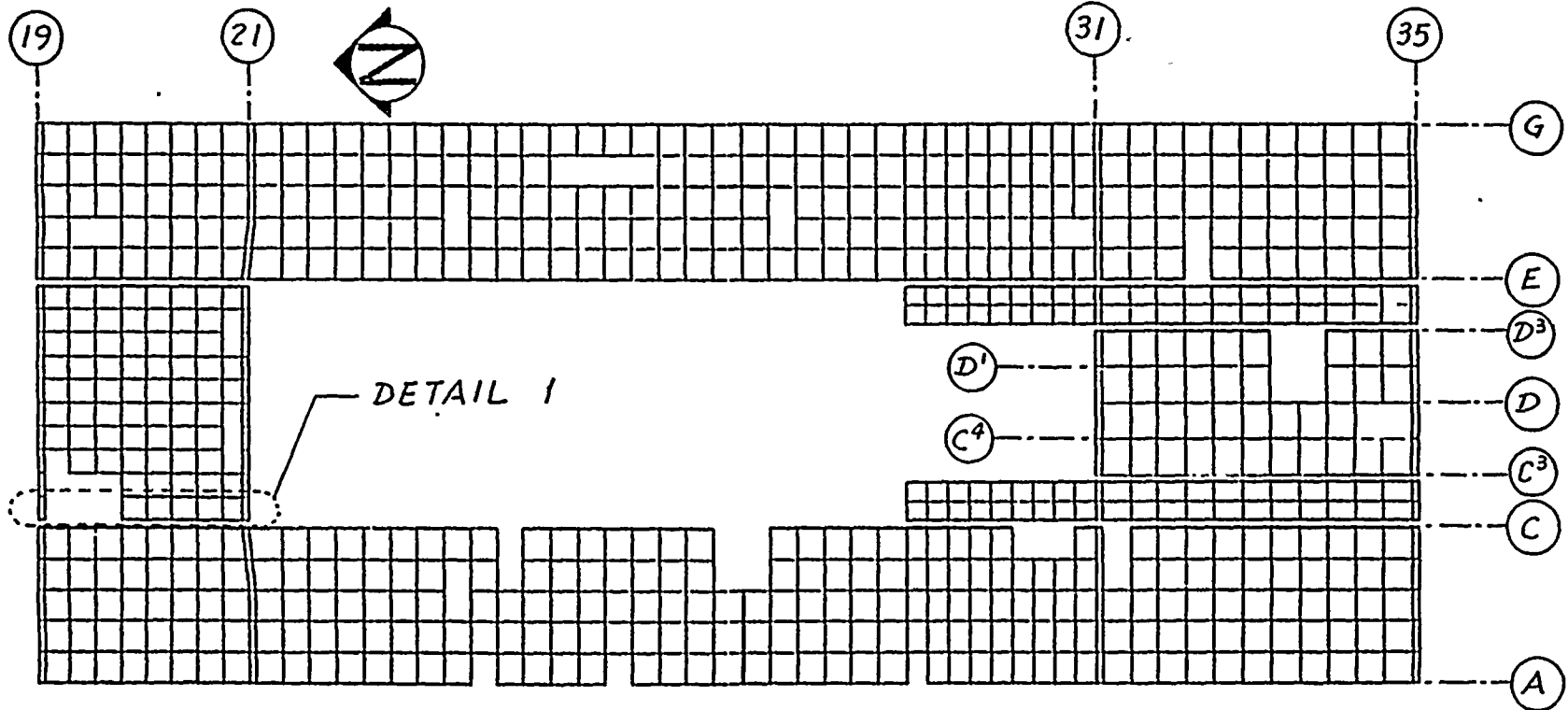


FIGURE 3 - UNIT 2 TURBINE BUILDING ELEV. 140 FT. FLOOR DIAPHRAGM
FINEL ANALYSIS MODEL



ATTACHMENT A
DESCRIPTION OF COMPUTER PROGRAM CE801 (FINEL)

Contents

Introduction
History of the Program
Applications
Program Features
Coordinate System and Sign Convention
Stress-Strain Laws
Output Description
Verification
References

Appendix A - Verification Problems



INTRODUCTION

The following sections contain a short description of Bechtel's computer program CE801-FINEL, with special emphasis on its application to the analysis of the reinforced concrete slab of the turbine building operating floor at Diablo Canyon Unit 2.

HISTORY OF THE PROGRAM

The original version of the program became available at the University of California, Berkeley, in 1962. Subsequently, the program was further developed by Wilson and Jones at Berkeley; their report (Ref. 1) describes the version which was acquired by Bechtel in the mid-1960s. This version was capable of analyzing axisymmetric solids with elastic-plastic materials.

These materials were represented by a bilinear stress-strain relation and a von Mises yield criterion for isotropic materials. Bechtel engineers implemented the following new features: restart capability, resultant section force and moment calculation, strain output option, two categories of materials, and special elements to represent steel reinforcing. In addition, improvements were made to the mesh generation and output plotting features, and concrete cracking was incorporated as a special case of elastic-plastic behavior.

In late 1972, extensive modifications were made that included improving program operating efficiency through program restructuring and applying a new equation solver, and the removal of problem size and bandwidth limitations.



An option was added to check for singularity in the stiffness matrix, and correct it, and the user was given more control over the contents of the output.

In October 1977, the stiffness matrix formulation was changed to use isoparametric quadrilateral elements instead of the original, constant strain, elements.

In September 1979, the von Mises criterion was extended to all materials in computing the failure envelope. Also, the change of the Poisson's ratio of the yielded materials was added.

APPLICATIONS

FINEL is a two-dimensional, static, small displacement, bilinear-elastic, finite element, stress analysis computer program. Solution is obtained through iteration. FINEL's primary purpose is to perform plane stress, plane strain, or axisymmetric stress analysis of reinforced concrete structures. The program allows for concrete cracking and yielding and reinforcement yielding. Loadings include concentrated, pressure, displacement, thermal, and inertial forces.

An R-Z-T coordinate system is used, R representing the radial direction, T the hoop direction, and Z the axis of revolution. The model of a plane problem is in the R-Z system (Figure 1).



FINEL has been used extensively to analyze reinforced concrete containment vessels, arch dams, underground cavities, and various structural elements.

PROGRAM FEATURES

1. Material Properties:

Two types of material behavior are incorporated into FINEL:

- a. Ductile: the stress-strain curve is bilinear in compression and bilinear in tension. This type of material is used to model reinforcing steel, steel plate, sliding surfaces, etc. (Figure 3).
- b. Brittle: the stress-strain curve is bilinear in compression and discontinuous in tension. This material is used to represent concrete, soil, etc. (Figure 4).

The von Mises yield criterion is used for ductile materials in tension and compression, and for brittle materials in compression. A material yields in all directions when the yield criterion has been exceeded. For the one-dimensional (reinforcement) material, maximum strain yield criterion applies. Yielding and unloading take place along the bilinear stress-strain curves.



A brittle material cracks (i.e., the stiffness is reduced to a small prescribed value) in the direction in which the principal stress has exceeded the fracture stress. A shear stiffness reduction factor is applied to materials which have cracked in only one direction, normal to the R-Z plane. If not otherwise specified by the user, the factor is 0.5. As the intent is to determine the cracking pattern that coincides with the principal directions of the strains, the importance of the shear stiffness tends to diminish.

Both categories of materials have temperature-dependent properties. Each material is isotropic in the R-Z plane before cracking, except in reinforcement type elements.

The Poisson's ratio of materials, other than those representing reinforcement, is increased as yielding increases, approaching 0.5 asymptotically.

2. Element Types:

The basic element type used in FINEL is linear and rectangular, as described in Reference 2, pp. 107-110. In addition to the basic element type, FINEL has a special quadrilateral element with unidirectional stiffness, used to simulate material such as reinforcing steel.



3. Section Resultant Forces:

The resultant forces at specified sections in the finite element model can be calculated.

4. Cycles, Load Factors, and Restart Capability:

Each analysis run consists of a specified number of analysis cycles, with each cycle defined by a set of possibly variable load factors which factor the input loads, the concentrated forces, two kinds of pressure loads, displacements, axial acceleration, and temperatures. Convergence is achieved when, between two successive cycles, the changes in element strains become negligible.

A restart tape can be created during the run, containing all the information for each cycle. Using this tape, the problem can be subsequently restarted at any cycle and continued for a specified number of additional cycles.

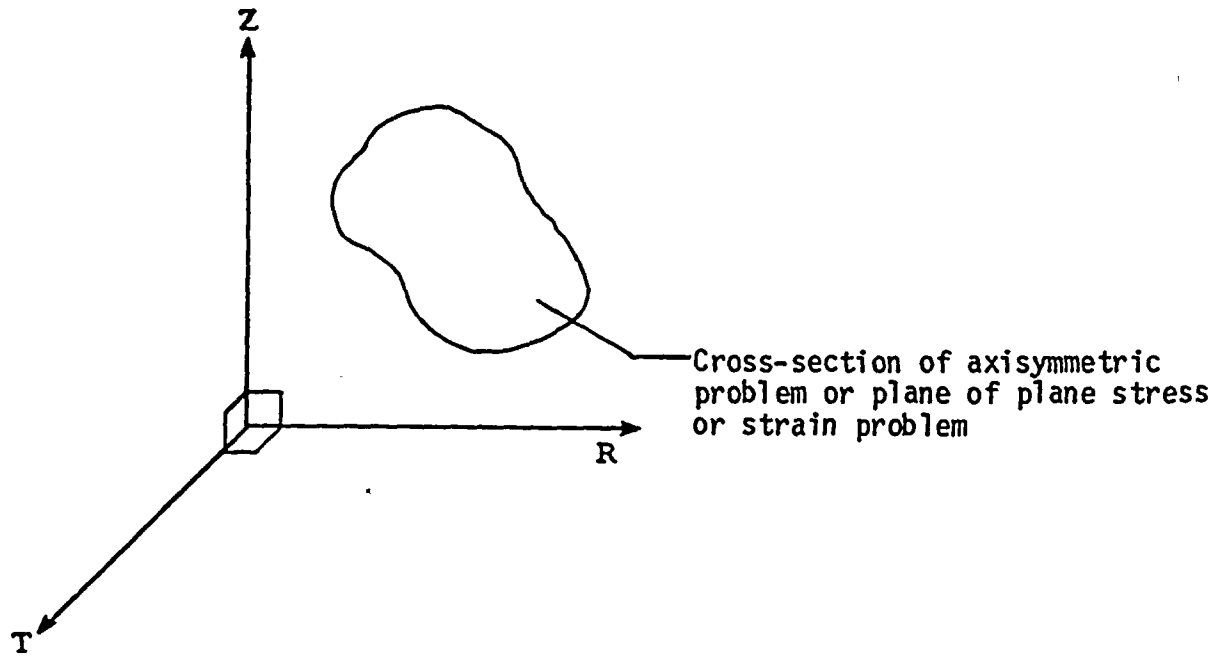
5. Plotting:

FINEL creates output files which can be read by the FPLOT program to produce plots of geometry, stress contour, strain contour, and principal direction plots.



COORDINATE SYSTEM AND SIGN CONVENTION

The structure coordinate system is shown in Figure 1 below. The stress sign convention is shown in Figure 2.



The element coordinate system is shown below:

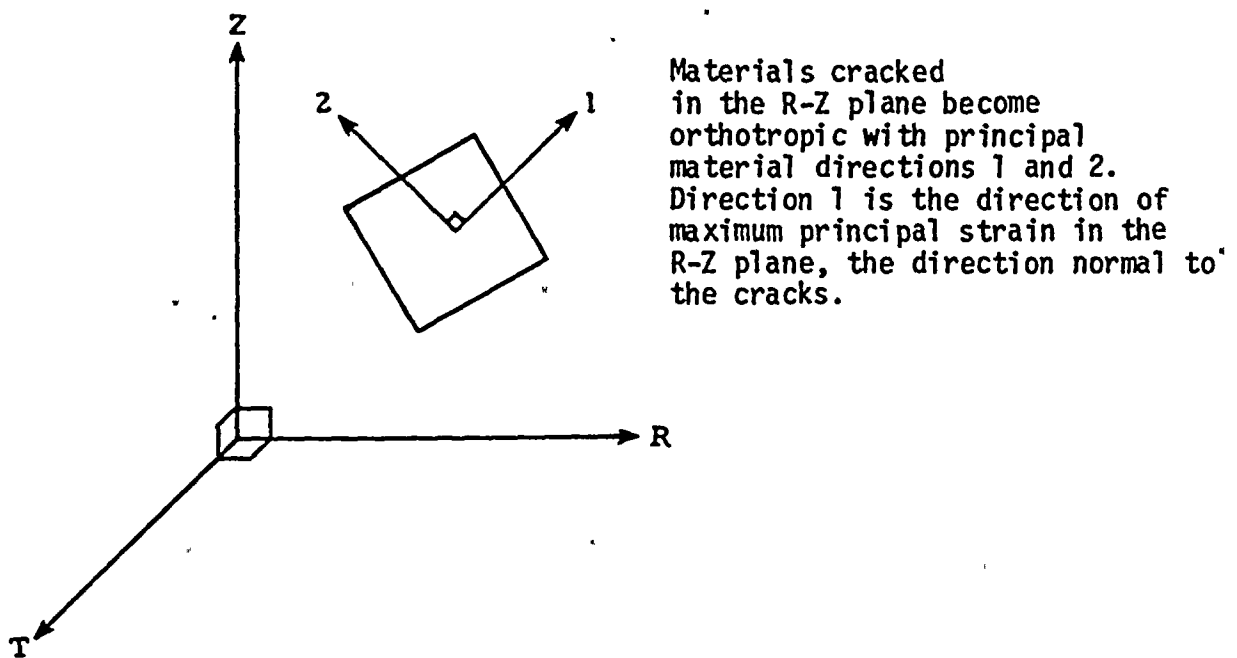


Figure 1. Coordinate System and Sign Convention



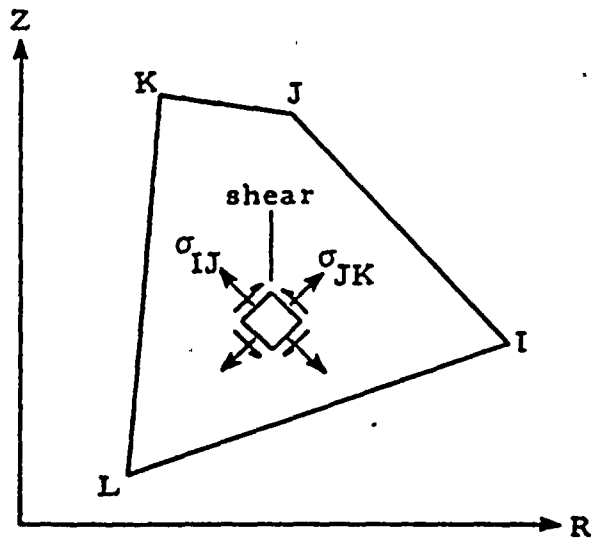
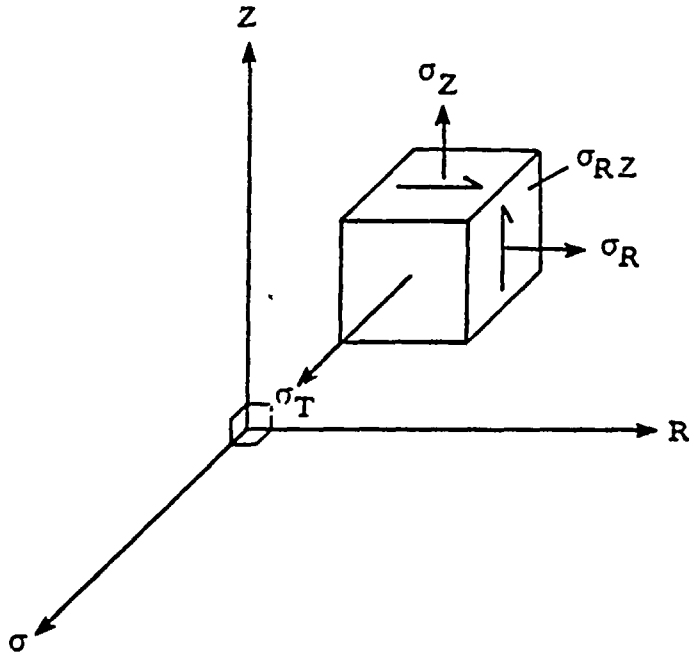


Figure 2. Stress Sign Convention



STRESS-STRAIN LAWS

1. Stress-strain Curves:

Ductile and brittle materials are considered in FINEL. Both have bilinear stress-strain properties in compression, but in tension one has bilinear properties, the other one is allowed to crack. The stress-strain curves are shown in Figures 3 and 4:

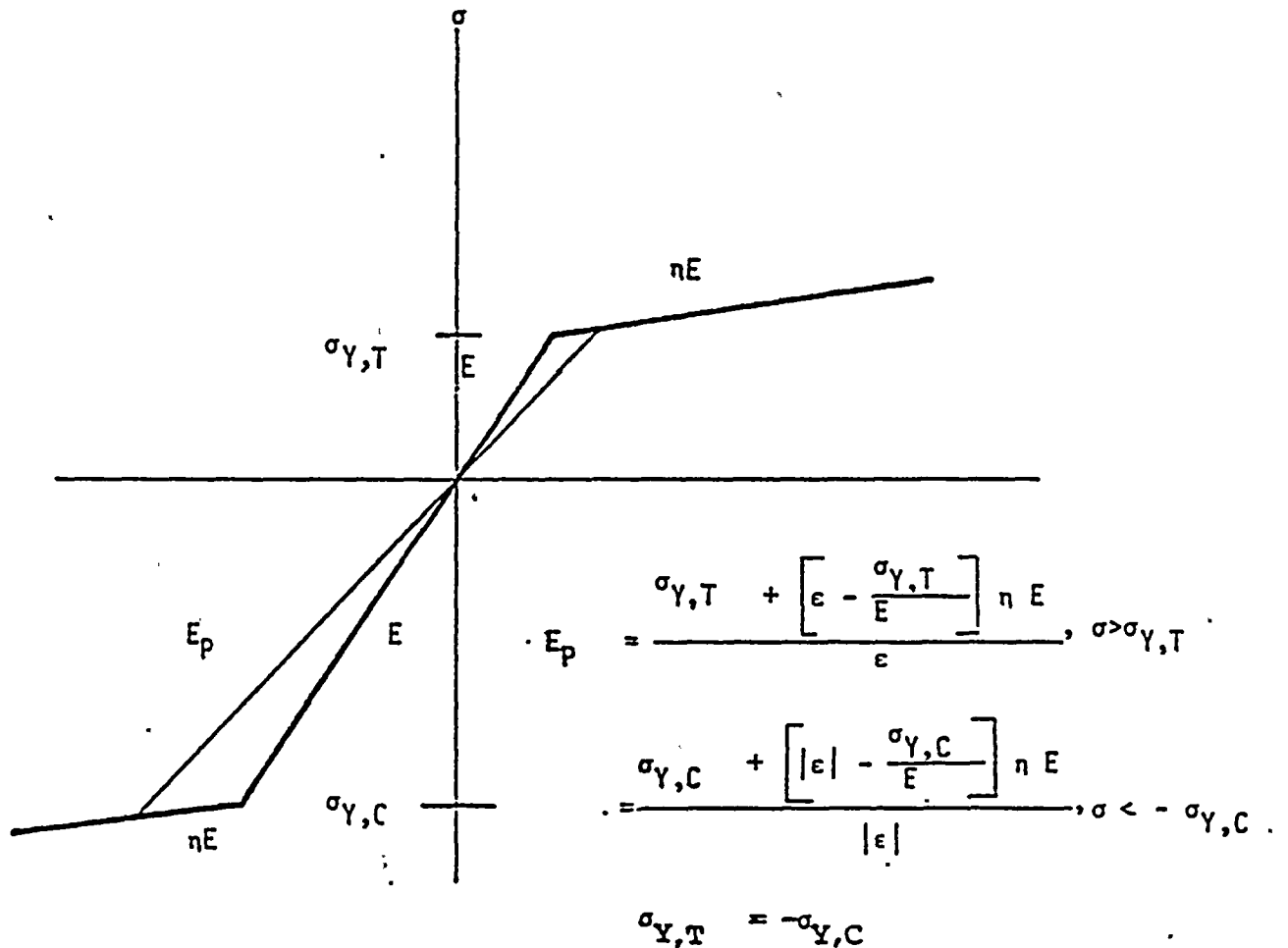


Figure 3. Stress-strain Curves for Ductile Material

Note: E = modulus of elasticity, σ = stress, ϵ = strain, η = modular ratio.
Indices: T = tension, C = compression, p = plastic, Y = yield



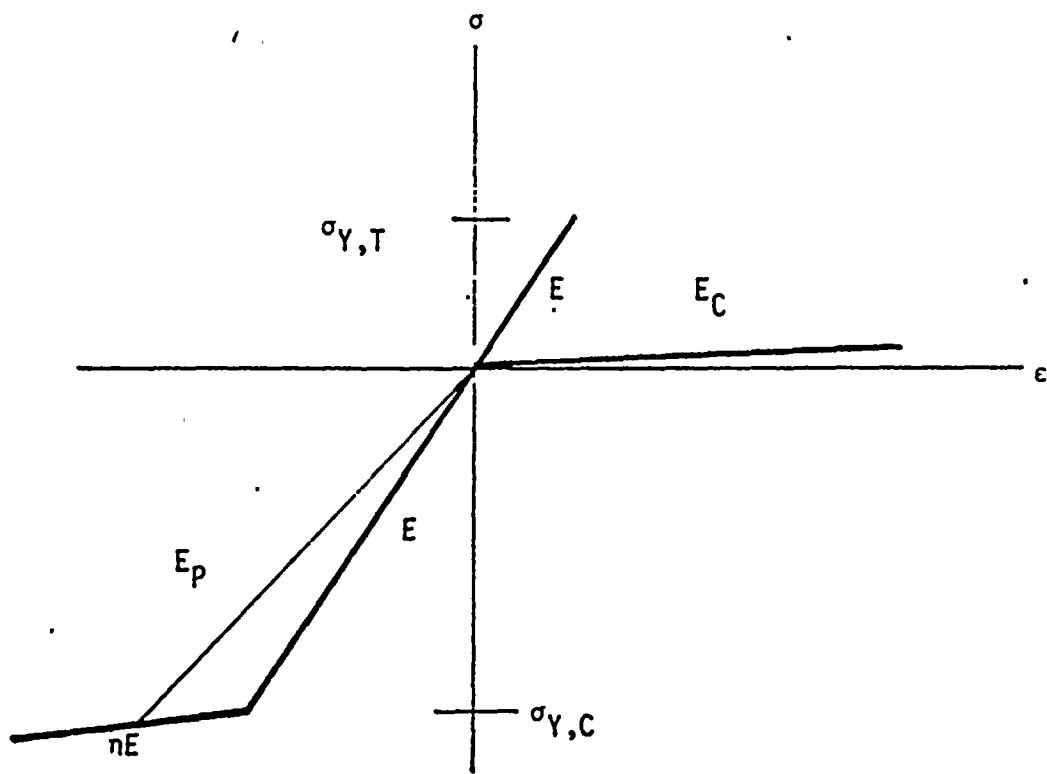


Figure 4. Stress-strain Curves for Brittle Material

NOTE: For a definition of symbols, see Figure 3.



2. Yield Criteria:

After the completion of each cycle of the analysis, the condition of the material of each element is reviewed and, if required, the material properties are redefined for the following cycle. The decision is based on the relation of the strain condition to the originally specified material properties, that is, equivalent stresses are used rather than stresses obtained in the preceding cycle.

One-, two-, or three-dimensional stress-strain conditions are considered. When yielding is indicated, the value of the new modulus of elasticity (E_p) is computed according to the stress-strain laws described above under Item 1.

Two-dimensional materials, such as used in a plane stress element, are defined by a stress ellipse (Figure 5). In case of brittle material the ellipse is terminated at the tensile strength in the tensile quadrants.

The long axis of the failure ellipse is $\sigma_{Y,C}\sqrt{2}$, while the short one is $b_y = \frac{\sigma_{Y,C}}{\sqrt{1.5}}$. The short axis of that ellipse on which lies the resultant of the two principal stresses is: $b = \sqrt{\sigma_2^2 + \sigma_3^2} \sqrt{\sin^2 \theta + \frac{\cos^2 \theta}{3}}$. If $|b| > |b_y|$, yield occurs, and new properties will be applied, b , and b_y representing σ and $\sigma_{Y,C}$, respectively.



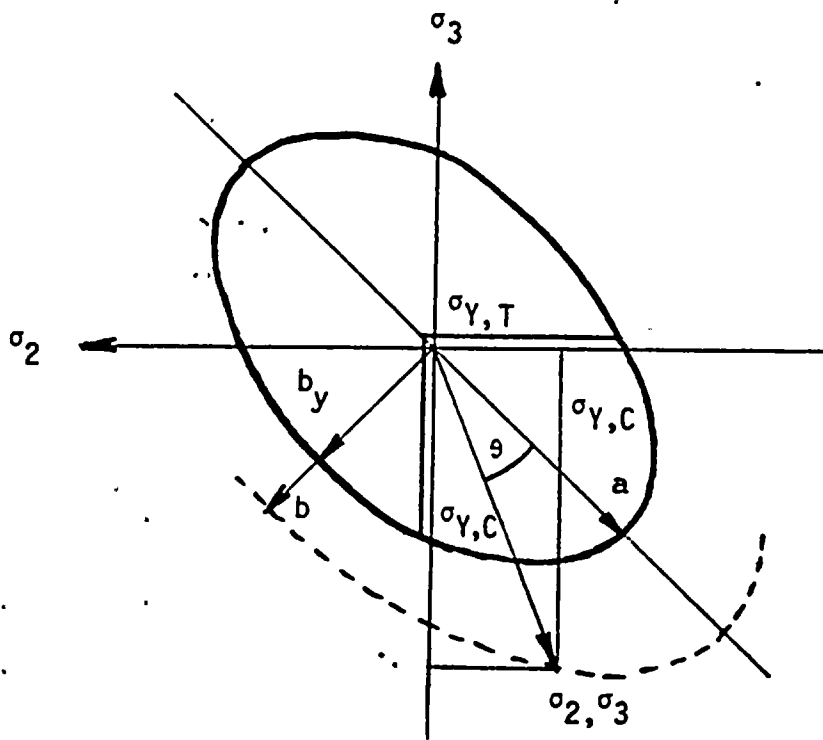


Figure 5. Two-dimensional Failure Criterion



Material specified as one-dimensional, such as reinforcement, or those that become one-dimensional by brittle tensile failure are checked simply according to their strain in the specified or principal direction, as applicable.

When a two- or three-directional material becomes plastic, the Poisson's ratio is increased. To avoid oscillation between the cycles, the value of the Poisson's ratio approaches 0.5 exponentially as the plastic flow increases:

$$\nu_p = .5 - (.5 - \nu)e^{\frac{E}{E_p} - 1}, \text{ when } \frac{E}{E_p} > 1.$$

3. Cracking of Brittle Material:

The program iterates to achieve a condition of the structure in which concrete resists only compressive stresses, while all tension is resisted by reinforcement. To facilitate convergence of the solution the user must specify a non-zero tensile strength of the concrete.

To achieve the above outlined condition, the concrete is assumed to crack in the direction normal to the tensile principal strain(s) in any given cycle of the iterative process, i.e., no assumed cracking pattern is specified by the user, and during the iteration no cracking condition is saved for more than one (immediately following) cycle. In this way, the model representing concrete cannot resist a significant tensile stress as a component of shear.



4. Evaluation of Cracking:

The stress-strain relationship is shown in Figure 6. In the first cycle of an analysis the concrete material is homogeneous and isotropic, although in the T direction it may have properties different from those in the R-Z plane, e.g., in case of a plane stress analysis, $V_t = 0$. At the end of the cycle the principal stresses in each element are compared to the tensile stress limit. If the maximum stress exceeds the tensile stress limit, the material of that element is considered cracked in the corresponding direction. The second direction is also examined for possibly excessive tensile stress, and if found to be cracked, the third direction is also examined, considering one-directional stress-strain relationship. The possibility of yielding in compression in the remaining uncracked directions as applicable is also checked.

Based on the result of the above screening, the condition of the material of the corresponding element is determined. The direction (β in Figure 6) of the principal axes relative to the R-Z coordinate system is also determined, if the material has become orthotropic.

The new material properties replace the original ones in the $[\bar{C}]$ property matrices shown in Figure 6, and after the applicable rotation the stress-strain relationship is established for the following cycle as shown in Figures 7a and 7b.



After the second and succeeding cycles, the procedure is repeated, always considering the strain condition of the element and the original properties, rather than the properties the material had at the beginning of the cycle.



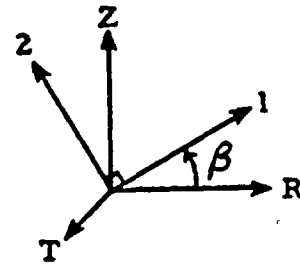
Stress-Strain Law - Orthotropic material

$$\{\epsilon\} = [C] \{\sigma\}$$

where,

$$[C] = [a]^T [\bar{C}] [a]$$

$$[\bar{C}] = \begin{bmatrix} C_{11} & C_{12} & C_{1T} & 0 \\ C_{12} & C_{22} & C_{2T} & 0 \\ C_{1T} & C_{2T} & C_{TT} & 0 \\ 0 & 0 & 0 & 1/G_{12} \end{bmatrix}$$



, constitutive equation

1 and 2 are principal material directions in R-Z plane

$$[a] = \begin{bmatrix} \cos^2\beta & \sin^2\beta & 0 & 2 \sin\beta \cos\beta \\ \sin^2\beta & \cos^2\beta & 0 & -2 \sin\beta \cos\beta \\ 0 & 0 & 1 & 0 \\ -\sin\beta \cos\beta & \sin\beta \cos\beta & 0 & \cos^2\beta - \sin^2\beta \end{bmatrix}$$

Figure 6. Stress-strain Matrices



Type 1 - Original Properties:

$$[\bar{C}] = \begin{bmatrix} \frac{1}{E_{R-Z}} & -\frac{\nu_{R-Z}}{E_{R-Z}} & -\frac{\nu_T}{2} \left(\frac{1}{E_{R-Z}} + \frac{1}{E_T} \right) & 0 \\ & \frac{1}{E_{R-Z}} & -\frac{\nu_T}{2} \left(\frac{1}{E_{R-Z}} + \frac{1}{E_T} \right) & 0 \\ & & \frac{1}{E_T} & 0 \\ & & & 2 \frac{1 + \nu_{R-Z}}{E_{R-Z}} \end{bmatrix}$$

Type 2 - Material cracked once parallel to direction T:

$$[\bar{C}] = \begin{bmatrix} \frac{1}{E_{C,R-Z}} & 0 & 0 & 0 \\ & \frac{1}{E_{R-Z}} & -\frac{\nu_T}{2} \left(\frac{1}{E_{R-Z}} + \frac{1}{E_T} \right) & 0 \\ & & \frac{1}{E_T} & 0 \\ & & & 2 \frac{1 + \nu_{R-Z}}{E_{R-Z}} \end{bmatrix}$$

Type 6 - Material cracked in all directions:

$$[\bar{C}] = \begin{bmatrix} \frac{1}{E_{C,R-Z}} & 0 & 0 & 0 \\ & \frac{1}{E_{C,R-Z}} & 0 & 0 \\ & & \frac{1}{E_{C,T}} & 0 \\ & & & 2 \frac{1 + \nu_{R-Z}}{E_{C,R-Z}} \end{bmatrix}$$

Figure 7a. Property Matrices



Type 8 - Plastic, one crack parallel to direction T:

$$[\bar{C}] = \begin{bmatrix} \frac{1}{E_{C,R-Z}} & 0 & 0 & 0 \\ \frac{1}{E_{P,R-Z}} & -\frac{\nu_{P,T}}{2} \left(\frac{1}{E_{P,R-Z}} + \frac{1}{E_{P,T}} \right) & 0 & 0 \\ \frac{1}{E_{P,T}} & 0 & 0 & 0 \\ 0 & 0 & 0 & 2 \frac{1 + \nu_{P,R-Z}}{\gamma E_{P,R-Z}} \end{bmatrix}$$

Figure 7b. Property Matrices



OUTPUT DESCRIPTION

1. Printed Output:

The printed output consists of the following:

- a. Reproduced input data: All the data cards are reproduced in the printed form. Note that the format for printing is different from that of the cards.
- b. Developed input data: The complete problem data is printed out. This includes the parameter listing, load factors, material properties, complete nodal point, element and boundary pressure information, and the section data. Maximum and minimum coordinates are also printed.
- c. Equation solution parameters: The parameters which control the storage in the block equation solver are listed. The parameters are:
 - o total number of equations
 - o maximum half-bandwidth
 - o number of equations per block
 - o number of blocks
 - o value of MTOT (required core storage)



2. Results:

If requested in the input, for each cycle the stresses and, if required, the strains for all elements are listed. This output consists of the stresses and strains in the R, Z, and T directions. Also, the maximum and minimum principal stresses and strains in the R-Z plane are printed together with the angle (R rotated into Z positive) in degrees from the R direction to the maximum stress and strain direction. Further, the stresses and strains acting on a section, parallel to the IJ face of each element and on a section normal to it, are printed. Figure 2 shows the stress sign convention. The code number of the material condition is printed before an element number unless it is the original one. In any cycle after the first one, the changes in strains relative to the previous cycle are printed, related always to the new principal directions.

If an element stiffness matrix will be changed in the following cycle as a result of cracking or yielding, a message appears following the stress and strain output of the element, indicating the material code applicable in the following cycle. The saved angle indicates the orientation of the maximum tensile principal strain (direction 1) relative to the axis R. Direction 2 is normal to Direction 1.

After the element stresses and strains the following additional information is given:



- a. The nodal point displacements and reactions
- b. Resultant forces at specified sections
- c. Maximum stress-strain values for each material
- d. Time log used by various parts of the program

Preceding the stress and strain information of each cycle, except the first one, the program will print a list of condition codes and properties for all elements whose stiffness matrix will be modified according to the condition code. An explanation of the code numbers is given before the first cycle.

Following the stress and strain information of the last cycle, the new codes and properties to be used in a restart case are listed, if they are different from the original ones.

VERIFICATION:

1. Analytical method:

The analytical method applied in FINEL in calculating concrete and reinforcement stresses, when the cracking of concrete in tension is considered, is essentially the same as described in Reference 10. The



validity of the analytical method applied in FINEL, when calculating stresses in concrete and reinforcement after concrete cracking, is supported by several test programs, such as conducted by the laboratories of the Massachusetts Institute of Technology, Cornell University, and the Portland Cement Association, and reported in several publications (Refs. 5-9). Reference 5, page 13 can be quoted: "Duchon has proposed a method through which the stresses and strains in both the steel and concrete are obtained. Once the stresses and strains have been calculated, they are checked against code allowables." And: "The most popular method of calculating stresses and strains in the concrete, and in the hoop, meridional, and diagonal reinforcing bars, resulting from forces obtained in the containment analysis, is that proposed by Duchon. The model is appropriate for loads larger than those that cause cracking in the concrete. The tensile strength of concrete and dowel forces in the reinforcing are neglected. It is applicable for internal pressure and/or seismic loads. The model predicts the highest probable stresses in each component element."

In Reference 6, page B-19, Figure B-14, repeated partly as Figure 8 in this report, an example can be seen of the behavior of the deformation of an orthogonally reinforced concrete test panel subjected to biaxial tension and monotonically increased shear force as well as many cycles of completely reversed shear loading. In that figure, as in several others placed in the same report, reference is made to the subject analytical



model, indicating reasonably close correlation between calculated and measured values when the loading approaches the capacity of the test specimen. It is also significant that, in the application of FINEL in analyzing the operating floor slab of the turbine building, the effects of the horizontal seismic responses are studied, which also should result in several load reversals, similar to the referenced test.



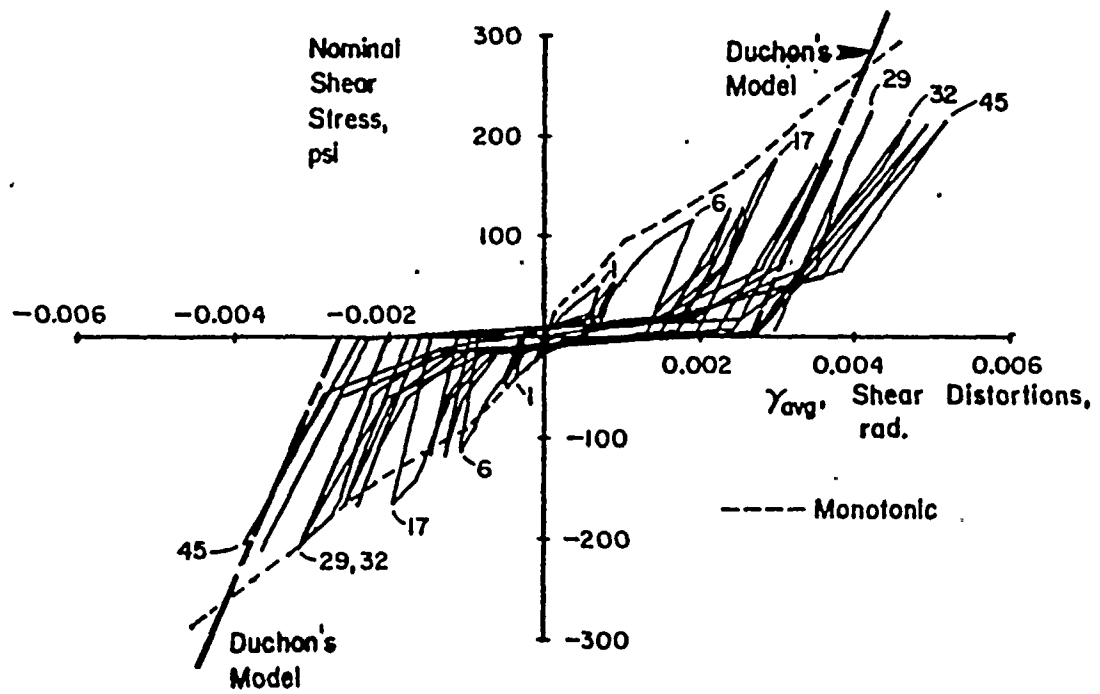


Figure 8. Average Measured Shear Distortion of a P.C.A. Test Specimen



2. FINEL Verification Runs:

In the FINEL Verification Manual, analyses of the following example problems are kept on record:

- A - Cracking analysis of a PCRV
- B - Analysis of a Simply Supported Beam
- C - Analysis of an End Loaded Cantilever
- D - Analysis of an Axially Constrained Hollow Cylinder with a Distributed Pressure Loading
- E - Analysis of an Axially Constrained Hollow Cylinder with a Linear Temperature Gradient
- F - Analysis of an Axially Constrained Hollow Cylinder with a Nonlinear Temperature Gradient
- G - Analysis of a Deep Elastic Panel
- H - Analysis of a Deep Elastic Panel (Finer Mesh)

These problems were analysed by FINEL and the results compared to tests or independent calculations.



Parts of the Verification Manual that are relevant to the present application of FINEL, problems C and H, are included in Appendix A.



REFERENCES

1. Wilson, Edward L. and Jones, Robert M., "Finite Element Analysis of Axisymmetric Solids with Orthotropic, Temperature-dependent Material Properties," Aerospace Report No. TR-0158(S3816-22)-1, September 1967.
2. Zienkiewicz, O. C., "The Finite Element Method," Engineering Science, McGraw-Hill, 1971.
3. Zienkiewicz, O. C., Owen, D. R. J., Phillips, D.V., and Nayak, G.C., "Finite Element Methods In The Analysis Of Reactor Vessels," Nuclear Engineering and Design, Vol. 20, No. 507, 1972.
4. Sozen, M. A. and Paul, S. L., "Structural Behavior of A Small-scale Prestressed Concrete Reactor Vessel," Nuclear Engineering and Design, Vol. 8, pp 403-414, 1968.
5. "Analysis of Reinforced Concrete Containment Vessels with Nonlinear Shearing Stiffness," C. H. Conley, R. N. White, P. Gergely, Cornell University, NUREG/CR-3255, April 1983.
6. "Shear Transfer in Large Scale Reinforced Concrete Containment Elements Report No. 2," R. G. Oesterle, H. G. Russell, Construction Technology Laboratories, Portland Cement Association, NUREG/CR-2450, December 1981.
7. "Analysis of Shear Transfer in Reinforced Concrete with Application to Containment Wall Specimens," P. Leombruni, O. Buyukozturk, J. J. Connor, Massachusetts Institute of Technology, NUREG/CR-1085, October 1979.
8. "Shear Transfer in Large Scale Reinforced Concrete Containment Elements Report No. 1," R. G. Oesterle, H. G. Russell, Construction Technology Laboratories, Portland Cement Association, NUREG/CR-1374, April 1980.
9. "Strength and Stiffness of Tensioned Reinforced Concrete Panels Subjected to Membrane Shear, Two-Way Reinforcing," P. C. Perdikaris, R. N. White, P. Gergely, Cornell University, NUREG/CR-1602, July 1980.
10. Duchon, N.B., Analysis of Reinforced Concrete Membrane Subject to Tension and Shear, ACI Journal, Proceedings Vol. 69, No. 9, September 1972, pp 578-583.



Appendix A
Verification Problems

Copies of the following two verification problems from the FINEL Verification Manual are attached:

C: Analysis of an End Loaded Cantilever

H: Analysis of a Deep Elastic Panel (Finer Mesh)



C.1 INTRODUCTION

The analysis of an end-loaded cantilever of prismatic section was performed to test the constant-strain finite elements. The results were compared to hand calculations.

C.2 PROBLEM DESCRIPTION

Figure C.1 illustrates the beam geometry and finite element mesh. The problem was treated by a plane stress analysis. The mesh contained 19 nodes and 96 quadrilateral constant strain elements.

C.3 PROBLEM PARAMETERS

Elastic Modulus = 30,000 ksi

Poisson's Ratio = 0.25

Cantilever Tip Load = 40 kips

Moment of Inertia = 144 in⁴

Cross Sectional Area = 12.0 in²

C.4 HAND CALCULATIONS

C.4.1 Bending Stresses

Using the following information, the bending stresses were calculated for various elements and tabulated in Table C.1.

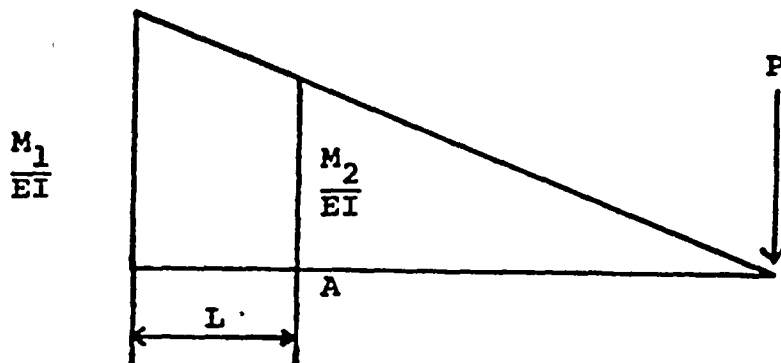
Boundary elements provide $y = \pm 5"$

Bending stress = My/I ksi = $\pm 5M/144$



C.4.2 Flexural Energy Deflections

The flexural deflections were calculated using the following information and tabulated in Table C.2.



$$\delta_A = \frac{M_1 L}{2EI} \left(\frac{2L}{3}\right) + \frac{M_2 L}{2EI} \left(\frac{L}{3}\right) = \frac{L^2}{3EI} \left(M_1 + \frac{M_2}{2}\right)$$

$$M_1 = 40K(48") = 1920 \text{ k-in}$$

C.5 COMPARISON OF RESULTS

The deflections and stress results from the FINEL program are compared with the hand calculations in Tables C.3 and C.4. The theoretical linear strain variation across the depth of the beam is represented by discrete constant strain "steps" due to these finite elements. The differences in results are largely due to this feature of the constant strain elements.

C.6 CONCLUSION

In the comparison of results, it can be seen that the FINEL solution compares quite well with the hand calculations. Therefore, the FINEL program is verified for this type of plane stress analysis.



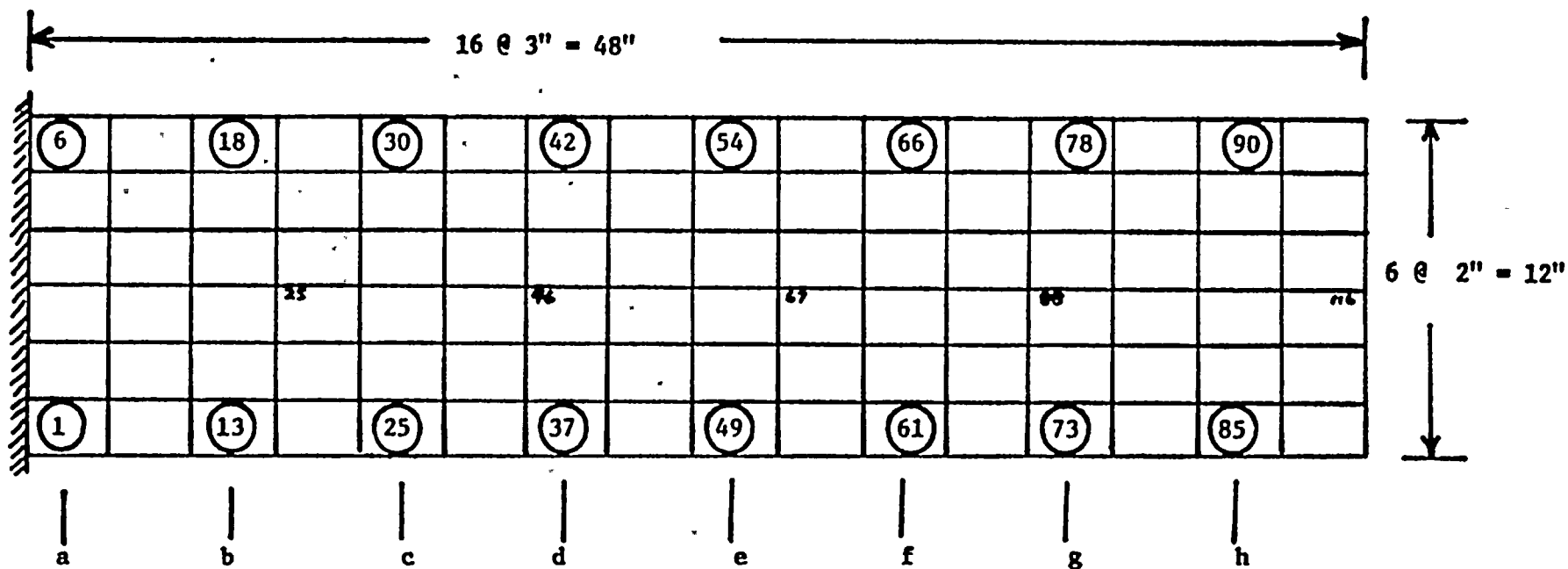
C.7 REFERENCES

- (1) C.A. Felippa, "Refined Finite Element Analysis of Linear and Nonlinear Two-Dimensional Structures", SESM Report No. 66-22, U.C. Berkeley Structural Engineering Laboratory, October 1966.

C.8 COMPUTER OUTPUT

The following is a copy of the computer output for the FINEL analysis of the end loaded cantilever used in this verification.





Parabolic Variation
of Tip Loading

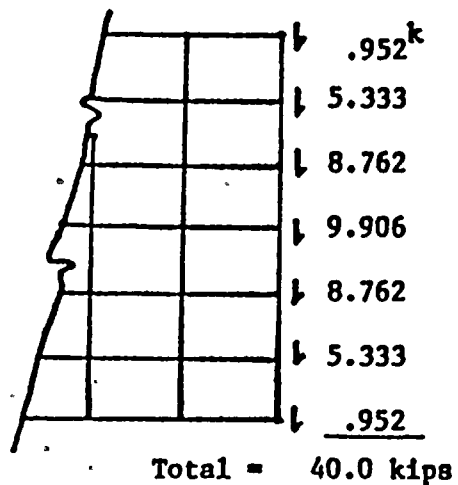


FIGURE C.1 Beam Geometry And
Finite Element Mesh

C-4



TABLE C.1 Bending Stresses
Of Various Elements

Elements	Bending Stress (ksi)
1 or 6	64.5833
13 or 18	56.2500
25 or 30	47.9170
37 or 42	39.5833
49 or 54	31.2500
61 or 66	22.9170
73 or 78	14.5833
85 or 90	6.2500

TABLE C.2 Flexural Stresses
At Various Node Points

Node	M_2 (k-in)	L (in)	$M_1 + M_2 / 2 = \alpha$	$\alpha L^2 / 3EI = \delta$
25	1560	9	2700	0.016875
46	1200	18	2520	0.063000
67	840	27	2340	0.131625
88	480	36	2160	0.216000
116	0	48	1920	0.341333



TABLE C.3 Deflection Results From FINEL
Verification Using An End-Loaded
Cantilever

Node	Deflections	
	FINEL	Hand Calculations
25	.0184	.0169
46	.0660	.0630
67	.1354	.1316
88	.2202	.2160
116	.3458	.3413

(Flexural deflections
only are computed here)

TABLE C.4 Stress Results From FINEL
Verification Using An End-Loaded
Cantilever

Section	Flexure Stress	
	FINEL	Hand Calculations
a	63.932	64.5833
b	54.705	56.2500
c	46.666	47.9170
d	38.548	39.5830
e	30.433	31.2500
f	22.317	22.9170
g	14.202	14.5830
h	6.074	6.2500

(Computed at center of
outer elements to
correspond to output
from computer)



H.1 INTRODUCTION

This verification compares the FINEL solution and a hand calculated solution for the stresses at two corners of a deep elastic panel subjected to a uniformly distributed load. The panel is the same one used in Appendix G and is shown in Figure H-1. However, in this case, a finer finite element mesh was used to show the change in accuracy of the results.

H.2 PROBLEM DESCRIPTION

The simply supported panel shown in Figure H-1 had a uniformly distributed load along the top edge of intensity p kips per unit length. The stresses at two of the corner points were calculated by extrapolating data obtained from FINEL and comparing it to a hand calculated solution to the equations of elasticity. Extrapolation was required because FINEL calculated stresses at the centers of the finite elements, but the values at the corners were needed for a comparison with the theoretical solution.

H.3 PROBLEM PARAMETERS

Thickness = $t = 1.0$ inch
Loading = $p = 100$ k/in
Young's Modulus = $E = 3 \times 10^4$ ksi
Poisson's Ratio = $\nu = 0.3$

H.4 HAND CALCULATIONS

H.4.1 Theoretical Solution

Consider the simply supported deep panel (shown in Figure H-1) loaded along its top edge by a uniformly



distributed load. Since the panel is symmetric about the y axis, only half of the panel was used for this analysis. Timoshenko and Goodier (Reference 1) report the following results:

The stress function along the unloaded upper side of panel is:

$$\phi = -0.4pax + 0.18 pa^2$$

The stress function along the loaded portion of the upper side is:

$$\phi = -p \frac{x^2}{2} + 0.1pa^2$$

It follows that:

$$(\delta x)_{\substack{x=0 \\ y=0}} = +1.268p = +126.8 \text{ ksi}$$

$$(\delta x)_{\substack{x=0 \\ y=a}} = -.488p = -48.8 \text{ ksi}$$

These results were obtained with a finite difference discretization employing a square grid having a spacing of $a/6$.

H.4.2 Calculations For The Extrapolation

The stresses from the FINEL program for the diagonal finite elements are listed in Table H-1. These stresses are at the centers of the elements on a diagonal. Corner values of stress at node points 1 and 21 were extrapolated by using the following cubic polynomial fit:

$$y = (a_0 + x(a_1 + x(a_2 + a_3x)))$$



The cubic polynomial was solved by using a time share program and the results were included in Table H-1.

H.5 COMPARISON OF RESULTS

The results from the FINEL solution for the corner stresses of the deep elastic panel are compared to those from the hand calculated solution in Table H-2. The difference between the two methods of solution for the stresses is 4.887% at node point 21, and 8.774% at node point 1.

H.6 CONCLUSION

This verification problem demonstrates the performance of the constant strain finite elements to solve an elasticity problem where shear effects are significant. These results confirm the known limitations of this type of element.

H.7 REFERENCES

- (1) Timoshenko and Goodier, Theory Of Elasticity, McGraw-Hill, Second Edition, copyright 1951, pp. 487-489.
- (2) Connor and Will, "Computer Aided Teaching Of The Finite Element Displacement Method"; MIT Research Report 69-23, February 1969, p. 196.

H.8 COMPUTER OUTPUT

A copy of the FINEL output for the analysis of the deep elastic panel with a finer mesh is attached at the end of this appendix.





Table H-1 FINEL Stresses Along
Selected Diagonals

Elements	Stress (ksi)	Elements	Stress (ksi)
191	-0.3867	190	-0.5328
172	-1.3796	169	-3.4611
153	-2.2122	148	-9.3433
134	-2.8222	127	-15.817
115	-4.2382	106	-17.560
96	-8.0442	85	-7.7982
77	-15.330	64	17.519
58	-25.185	43	53.561
39	-35.674	22	90.635
20	-46.130	1	124.050
Extrapolated value at node 21	-51.185	Extrapolated value at node 1	137.925



Table H-2 Comparison Of Results
For The Deep Elastic Panel

Node	Stress	
	FINEL	Hand Calculations
21	-51.185	-48.8
1	137.925	126.8

